

Surface Analysis of Excimer-Laser-Treated Polyethylene-Terephthalate by Surface-Enhanced Raman Scattering and X-Ray Photoelectron Spectroscopy

TH. LIPPERT, F. ZIMMERMANN, and A. WOKAUN*

Physical Chemistry II, University of Bayreuth, D-95440 Bayreuth, Germany

Silver and gold island films have been evaporated onto various polymer surfaces; the samples were characterized by surface-enhanced Raman spectroscopy (SERS), UV-visible spectroscopy, and x-ray photoelectron spectroscopy (XPS). Among the series of investigated polymers, the SERS spectra recorded on stretched polyethylene-terephthalate (PET) foils are unique with respect to resolution and intensity; the signal strengths are comparable to those observed in enhanced *resonance* Raman scattering. This exceptional behavior is attributed to the semicrystalline nature of the investigated material, and to the preferred interaction of the deposited silver with carbonyl groups of the polymer. The formation of a metal/polymer bond was established by the observation of corresponding bands in the XPS spectrum. Upon melting or amorphization of PET, the SERS intensities are reduced; this result is attributed to a decrease in the metal/polymer bond strength, due to changes in orientation of the phenyl rings and of the carbonyl groups on the polymer surface. The PET surfaces have been modified by excimer laser irradiation at the wavelengths of 308 and 248 nm. The characteristic laser-induced structuring of the surface, as revealed by scanning electron microscopy, is related to the biaxial stretching applied during production of the PET foils, and has been studied for various orientations of the samples and different laser fluences. As a consequence of irradiation, a loss of oxygen is detected by a decrease of the C 1s XPS bands assigned to carbon atoms with singly or doubly bound oxygen, and by an overall decrease of the oxygen-to-carbon ratio. The surface polarity is observed to decrease, as accompanied by a red shift of the absorption maximum for silver island films deposited onto the irradiated surfaces. SERS spectra recorded on these samples are weaker in intensity, as compared to those recorded on untreated PET foils. This decrease is interpreted in terms of partial amorphization of the sample accompanied by polymer reorientation, loss of the preferred anchoring sites for nucleation of silver islands, and changes in the surface structure and morphology.

Index Headings: Polymers, surface analysis; Silver island films, polymer decoration; Contact angle measurements; Raman spectroscopy; Surface analysis, UV-visible spectroscopy; Laser surface modification of polymers; Surface-enhanced Raman scattering (SERS) of polymers; Scanning electron microscopy (SEM) of polymers; X-ray photoelectron spectroscopy (XPS) of polymers.

INTRODUCTION

Applications of surface-enhanced Raman scattering (SERS)¹⁻⁶ to polymers have proceeded along either path of two complementary routes. In the first approach, aimed at studying properties of the individual polymer molecules, macromolecules are adsorbed from solution onto silver electrodes,⁷⁻⁹ colloids,^{10,11} or island films.^{12,13} In the second class of investigations, which focuses on the specific properties of polymer surfaces, a silver island film is deposited on top of the solid polymer sample of in-

terest. This "silver decoration technique" is the subject of the present study.

In an early investigation,¹⁴ a polystyrene layer was deposited onto a silicon substrate by spin coating, and decorated by thermal evaporation of 4 nm of silver. In the resulting spectra, bands due to graphitic carbon were observed between 1200 and 1600 cm⁻¹. The appearance of graphitized product was attributed to a silver-catalyzed photo-oxidation of the polymer during the measurement.¹⁵ In a step to avoid this degradation, the polymer to be investigated was overcoated with a second thin polymer film.^{13,15} Various carbon materials have been characterized by Ag island film deposition and SERS measurements by Ishida *et al.*¹⁶

A related study¹⁷ used the deposition of a silver island film onto an ATR prism to enhance the sensitivity of FT-IR/ATR detection of polysiloxane and polycarbonate overlayers on polyethylene-terephthalate (PET) foils. Applications of silver decoration techniques for the SERS detection of adsorbates on inorganic substrates include the work of Mo *et al.*¹⁸ and of Van Duyn *et al.*¹⁹ on GaAs and silicon, and of Kaul *et al.*²⁰ on derivatized SnO₂.

Besides the analytical applications mentioned so far, the metallization of polymers is, of course, of high importance in materials science and in information technology. An overview on the use of metal layers on polymers for information storage has been given in Ref. 21. For example, in the fabrication of polymer-supported thin metallic films in video tapes, UV laser treatment has been used to enhance the adhesion, which determines the lifetime of the product.²² Micrometer resolution has been reported for the ablation of thin metallic films on polymers with the use of a XeCl* excimer laser.²³ Laser-induced desorption of metal from metallized polymers has been achieved with single pulses at wavelengths of 193, 248, or 351 nm, e.g., for aluminum on PET.²⁴ Depending on laser fluence, the ablation process either affects only the metal overlayer or comprises underlying polymer layers in addition.

In a study of aluminum deposition on PET, Sylvain *et al.*^{25,26} have concluded that the first layer of the metal contacting the polymer is fully oxidized. This factor is a consequence of the high heat of formation of aluminum oxide (-1650 kJ mol⁻¹), and appears to be a general result. In an XPS study of copper on PET, Chtai *et al.*²⁷ obtained evidence for a Cu-O-C bond, as will be discussed below in comparison with our results with deposited silver.

In the present report, several polymers are compared with regard to the quality of spectra obtained with the

Received 3 June 1993.

* Author to whom correspondence should be sent.

use of the silver decoration technique. High-sensitivity spectra are recorded on PET foils. The status of the surface is probed before and after excimer laser treatment. Changes are interpreted by using results from contact angle measurements, electron micrographs of the irradiated surfaces, x-ray photoelectron (XPS), and UV spectroscopy.

This information is relevant in view of recent laser ablation and UV treatment studies of PET surfaces. In particular, diverging results have been reported in the literature regarding the changes in surface oxygen concentration as a consequence of UV treatment. Upon irradiation at 185 nm with a Hg lamp, an increase of surface oxygen was detected by XPS.^{28,29} In contrast, upon irradiation with a single excimer laser pulse at 193 nm (of 100 or 450 mJ cm⁻² fluence), a reduction of the surface oxygen content was observed with the same technique.^{28,29} In a more extensive exposure to 100 pulses at 193 nm, Chtaib *et al.*³⁰ found the oxygen signal to decrease at fluences between 5 and 20 mJ cm⁻² per pulse; and oxygen increase was observed in the fluence range from 20 to 50 mJ cm⁻², whereas at even higher fluences the O1s signal resembled the one of the fresh PET surface.

For 248-nm irradiation with a single pulse of 145 mJ cm⁻² fluence, reduction of oxygen and loss of CO and CO₂ was detected by ATR/FT-IR.³¹ In contrast, Bahners *et al.*³² report an XPS-observed increase in the C=O signal subsequent to exposure of PET to 100 pulses of 90 mJ cm⁻² fluence at 248 nm.

Dyer *et al.*³³ have studied the products desorbing upon treatment of PET at the XeCl* excimer laser wavelength of 308 nm. Below the threshold for ablation (which amounts to 170 mJ cm⁻² at 308 nm and to 30 mJ cm⁻² at 248 nm), they detected small quantities of desorbing CO and traces of CO₂, but no benzene. Above threshold, a prominent loss of C=O and, in addition, significant amounts of CO₂ and benzene have been detected.³³

For irradiation of PET with one pulse of 180 mJ cm⁻² fluence, a surface temperature of ≈2000 K has been calculated.³⁴ While the virgin surface of PET foils exhibits glass-like smoothness, a controlled roughening has been observed as a consequence of 193-nm and 248-nm irradiation. The morphology of the created structures has been related to the stretching direction and the degree of crystallinity.³⁵ After laser treatment, a broadening of the XPS core-level signals (C 1s and O 1s) due to cross-linking or roughening of the surface is observed as a general feature.³⁶

EXPERIMENTAL

The PET foils (of 250, 100, 23, 12, and 6 μm thickness) were purchased from Goodfellow, and were used without further purification. The foils are biaxially oriented according to the manufacturer's specifications.

Samples were irradiated with the use of pulses from either of two excimer laser systems (Lambda Physik). Pulses of 100 mJ energy and 20 ns duration at 308 nm from a XeCl* laser (Model LPX 120i) were delivered to the sample at rates of 2 Hz (10 or 100 pulses) or 10 Hz (1000 pulses) in ambient atmosphere. In other experiments, samples were irradiated at a rate of 2 Hz with

100 pulses of 50-mJ energy and 25-ns duration at 248 nm, derived from a KrF* laser (Model LPX 105e).

Silver (99.99% purity) for the preparation of island films was purchased from Balzers. Silver island films of 5 nm mass thickness were prepared by slow thermal evaporation (0.3–0.6 nm/min) onto the polymer sheets in a bell jar chamber (Balzers, Model BA 360, vacuum 3 × 10⁻⁶ mbar). The average mass thickness (mass per area) of the film and rate of silver deposition were measured with a 6-MHz quartz crystal microbalance (film thickness monitor, Balzers, Model QSG 301).

IR spectra were recorded on an FT-IR instrument (Perkin-Elmer, Model 1605). With the thinnest PET foils (6 μm thickness), spectra were recorded in transmission. Alternatively, the material was diluted by the silicon carbide sampling technique; the polymer surface was abraded with a silicon carbide substrate (LOT), and the latter placed into a diffuse reflectance cell (Spectra-Tech). Typically, 150 scans have been coadded for each spectrum at a resolution of 4 cm⁻¹.

For normal Raman scattering, the polymers were excited by the 530.9-nm line of a krypton-ion laser, with the use of 13 mW of power. Raman signals were dispersed in a triple spectrograph (SPEX, Model 1877A), and detected with an optical multichannel analyzer based on a cooled photodiode array. The resolution of the triple spectrograph was set at 6.0 cm⁻¹. Signal accumulation times on the diode array were adjusted between 40 and 100 s, depending on signal strength; 10 to 20 exposures were accumulated for each spectrum. In the SERS measurements, 1.6 mW of power was focused onto a 150-μm-diameter circular spot. As these experiments were carried out in ambient atmosphere, we expect the outer surface of the silver islands to be covered by oxygen.

UV-visible spectra of the silver island films on the polymers were recorded in transmission on a Perkin-Elmer instrument (Model Lambda 19). Contact angle measurements were performed on a Krüss instrument (Model G40) with the use of ethylene glycol and water as the test fluids.

XPS experiments were performed on a Leybold instrument equipped with a 200-mm hemispherical analyzer (Model EA 11); the pass energy was set to 50 eV. A Mg K_α source (operating conditions: 10 kV, 10 mA) has been used for excitation.

RESULTS

Raman Measurements on Untreated PET Foils. The Raman spectrum of a PET sample of 100 μm thickness is shown in the bottom trace of Fig. 1. Upon recording of the spectra from PET foils of different thicknesses, a perturbing fluorescence background was observed, the intensity of which increased with sample thickness. The best signal-to-noise ratio was therefore obtained for the 6-μm film; Raman signals could no longer be discerned on top of the fluorescence background for the 250-μm-thick sample. All Raman bands were assigned in agreement with the literature^{37–40} and are compiled in Table I.

SERS of PET Decorated with Silver and Gold Island Films. Upon deposition of a silver island film (5 nm mass thickness) onto the PET surface, the fluorescence background is completely quenched, in agreement with the

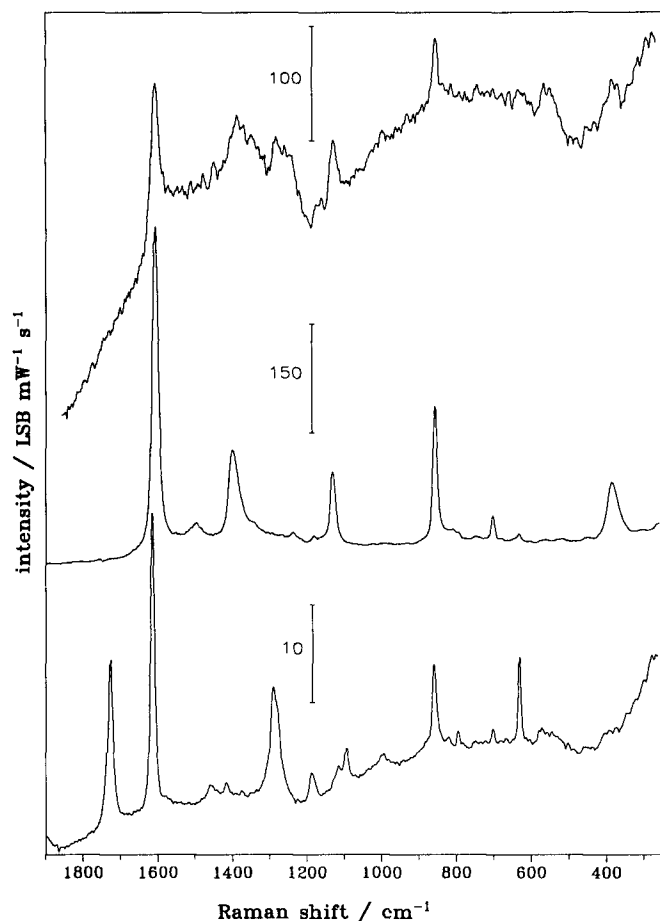


FIG. 1. Raman spectra from polyethylene-terephthalate (PET). Bottom: normal Raman spectrum from 100- μm -thick foil; middle: SERS spectrum from 6- μm -thick foil decorated with silver island film recorded in ambient atmosphere; top: SERS spectrum from molten 250- μm -thick foil with silver islands. Intensities recorded on the diode array multichannel detector (in least significant bits, LSB) are normalized with respect to excitation power at 530.9 nm (in mW) and integration time (in s); details are given in the Experimental section.

accepted model for the electromagnetic enhancement mechanism.⁴¹ As a consequence, it was possible to record SERS spectra from silver-decorated foils of all available thicknesses. Remarkably, the signal intensity was independent of sample thickness, as shown in Fig. 2. This observation demonstrates that the SERS spectrum predominantly originates from the enhanced signals generated in the surface region of the polymer.

The normal Raman spectrum from a 100- μm -thick PET sheet is compared with the SERS spectrum from a 6- μm foil in Fig. 1. The intensity enhancement becomes obvious upon observation of the calibration bars. New bands appearing in the SERS spectrum are assigned to IR-active PET modes, which acquire Raman activity due to the modified selection rules relevant for SERS. Some of the Raman-active vibrations observed in the normal spectrum (bottom) are missing in the SERS spectrum (middle trace).

Particularly noteworthy is the absence of the C=O stretching band at 1727 cm^{-1} . The latter effect might be explained in terms of SERS selection rules⁴² if the C=O group were oriented parallel to the surface, which would result in weak or no enhancement. As a second hypoth-

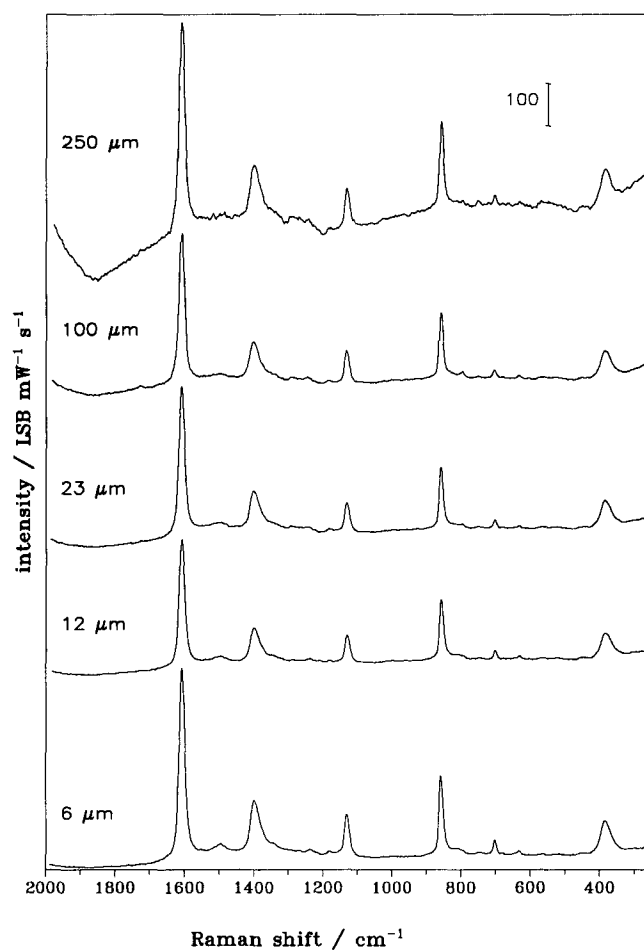


FIG. 2. SERS spectra from silver-decorated PET foils of various thicknesses, as indicated in the figure. Spectra were excited with the use of 1.6 mW of laser power at 530.9 nm. The calibration bar corresponds to 100 $\text{LSB mW}^{-1} \text{s}^{-1}$.

esis, we consider the formation of a C=O \cdots Ag bond, which would cause a substantial downshift of the C=O stretching frequency into the spectral range of C-C stretches, as has been previously observed for polyvinyl acetate by Lee and Meisel.¹⁰ A decision between these possibilities from the SERS spectrum alone is not possible. However, definite evidence for the existence of the silver/oxygen bond is obtained from XPS, as described below.

In an effort to demonstrate that the disappearance of the C=O stretching band is due to a frequency downshift, and to identify its shifted position, we have attempted to record SERS spectra from PET foils decorated with gold island films of 5 nm mass thickness, using 647-nm excitation. In case of formation of a C=O \cdots Ag bond, one would expect a different frequency shift of the C=O oscillator, and hence the reappearance of the band at a different position in the spectrum. Unfortunately, no enhancement of the Raman signals was observed for PET foils with gold island films. This observation may be correlated with the intrinsic instability of gold oxides, as expressed by a positive heat of formation.

Silver Decoration of Other Polymer Surfaces. To assess the potential of the silver decoration technique as a general tool for the characterization of polymer surfaces, we

TABLE I. Vibrational frequencies observed in IR, Raman, and SERS spectra.^a

Raman ^b (cm ⁻¹)	Raman ^c (cm ⁻¹)	(int.) (a.u.)	SERS ^c (cm ⁻¹)	(int.) (a.u.)	IR ^b (cm ⁻¹)	IR ^c (cm ⁻¹)	Assignment ^b symmetry
1727 s	1728	(16.2)			1724 vs	1724 vs	C=O st A _g ; IR: B _u
1613 vs	1615	(31.1)	1607	(469)	1613 vw	1612 vw	C=C st, ring, A _g
	1578	(1.0)	1557	(13)	1579 vw	1578 m	C-C st, ring, B _{3g}
			1497	(32)	1510 w	1503 m	C-C st, ring, B _{1u}
1458 vw	1456	(2.1)			1455 m	1453 m	Ra: CH def, glycol ^d mainly amorphous; IR: CH ₂ bend, A _g + B _u
1414 w	1417	(1.7)	1403	(70)	1414 m	1409 s	C-C st, ring, B _{2u}
			1392	(70)	1405 w		C-OH def, end groups ³⁸
1374 vw	1381	(1.0)	1359	(35)	1375 vw	1372 w	CH ₂ wag, A _g
	1337	(0.6)			1343 m	1338 m	CH ₂ wag, B _u
1290/ 1286 vs	1293	(2.9)	1278	(8)	1290-	1287/	Complex: ring and O-C st
	1286	(10.6)	1235	(14)	1240 vs	1239 vs	
1183 vw	1188	(2.6)	1180	(12)	1173 w	1175 w	CH in-plane bend, ring A _g
	1177	(1.7)					
	1134	(0.6)	1131	(101)		1133 - 1090 vs	Complex: CH in-plane bend, B _{2u} + C-O st, B _u
1118 m	1118	(2.7)			1124 vs		
1097 m	1096	(4.4)			1096 vs		
~1000 vw	1010	(0.9)			1039 w	1037 w	C-C st, glycol, A _g
	997	(1.0)				1018 s	CH in-plane bend, ring, B _{2u}
886 w	884	(0.2)			894 vw, sh	896 vw	CH ₂ rock, glycol A _u , amorphous
857 s	859	(8.5)	858	(179)	847 w	846 vw	C-C breathing, A _g
			851	(27)			
	823	(0.8)	811	(15)			
796 w	796	(1.5)	794	(4)	791 w	794 w	CH out-of-plane, ring; Ra: B _{1g} ; IR: B _{2g}
			746	(7)	727 vs	730 s	C-C in-plane bend ring, B _{2u} , and CH out-of- plane, ring, B _{3u}
704 vw	703	(1.5)	703	(36)			C-C-C out-of-plane, ring, B _{2g}
	669	(0.4)	680	(4)		669 vw	C-C-C out-of-plane, B _{3g} ³⁸
			641	(6)			C=O def, B _{3g} ³⁸
632 s	632	(8.7)	633	(7)	630 vw	632 vw	Ra: C-C-C in-plane bend, ring, B _{3g} ; IR: C=O wag B _{3u} ³⁸
			561	(2)	566 m		
			520	(4)	520 m	522 sh	C=O delta, B _{1u} ³⁸
			455	(4)	437 m		C-O-C bend
			385	(73)	382 s		CH def out-of-plane ring, B _{3u}
			360	(11)			

^a Note: s = strong; vs = very strong; vw = very weak; m = medium; w = weak; sh = shoulder.

^b References 37-40.

^c This work.

^d O-CH₂-CH₂-O fragment.

have carried out analogous experiments with other polymers. With *polypropylene*, an inelastic scattering background and impurity bands appear in the spectrum upon silver deposition, while the polymer bands have largely disappeared. On *PMMA* foils and *Teflon*[®] sheets, the intensity of the Raman bands stays essentially unchanged upon deposition of the island film; again, an inelastic background and impurity bands are observed. With *polyimide*, a strong fluorescence prevents the observation of Raman signals for the as-received foils. Upon silver decoration, the fluorescence is somewhat reduced, and Raman signals start to appear with a very poor sig-

nal-to-noise ratio, S/N ≤ 2. With *polystyrene*, the intensities of several Raman bands are increased by a factor of ≈ 2.5 as compared to plaques without silver; again, a strong fluorescence background and impurity bands appear in the spectrum.

The exceedingly high enhancement of the PET Raman signals obtained for the samples used in the present study, as compared to other polymers, might be due to the semicrystalline character⁴³ of the biaxially stretched PET foils. As a test of this hypothesis, a 250-μm-thick foil was placed onto a microscope slide, melted on a heating stage, and resolidified. Upon melting of the films, the stress-

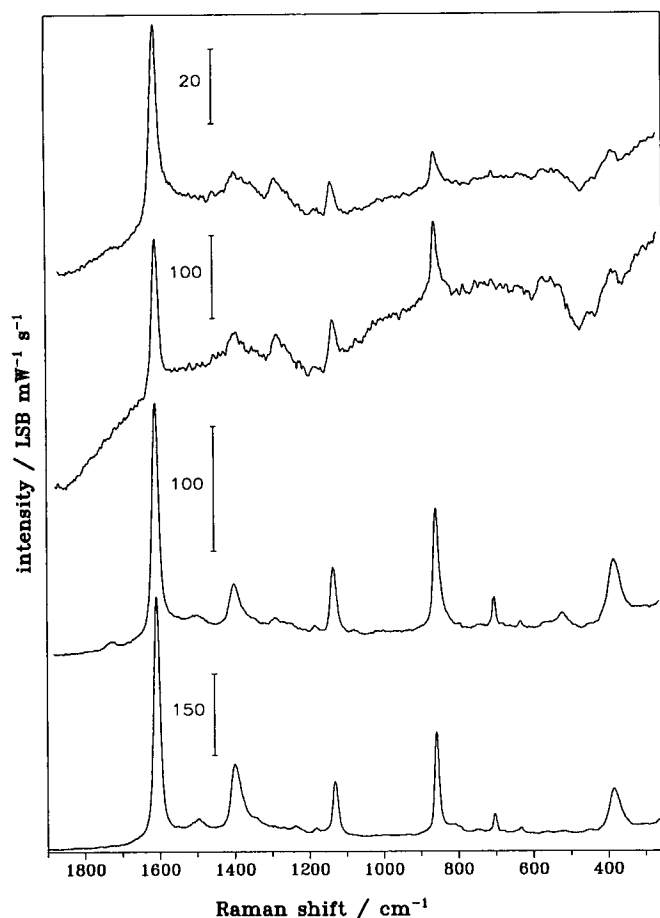


FIG. 3. Influence of excimer laser irradiation on the SERS spectra. PET foils (100 μm) were irradiated with excimer laser pulses, followed by silver decoration and recording of the Raman spectrum. Bottom trace: reference SERS spectrum of an unirradiated 6 μm PET foil; second trace: 100 pulses at 308 nm, 100 mJ incident onto 2 cm^2 area, rate 2 Hz; third trace: 1000 pulses at 308 nm, 100 mJ incident onto 2 cm^2 area, rate 10 Hz; top trace: 100 pulses at 248 nm, 50 mJ incident on 1.0 cm^2 area, rate 2 Hz.

induced orientation is lost, and an amorphous material results. The samples were decorated with Ag island films as before, and Raman spectra were recorded. In contrast to the untreated samples, only weak SERS signals and a high fluorescence background were detected (top trace in Fig. 1). This observation supports the idea that sample orientation effects are relevant for the observation of strong enhancement, as discussed below.

SERS Studies of PET Surfaces Modified by Laser Irradiation. In an examination of the potential of SERS for the detection of surface modifications of polymers, the PET foils were irradiated with excimer laser pulses at wavelengths of 308 and 248 nm, respectively. A series of pulse energies was chosen below and above the threshold for laser-induced ablation.^{33,44,45} Silver was evaporated onto the samples immediately after the laser treatment. Upon deposition of silver island films onto samples irradiated in this manner, the visible color of the film was observed to vary across the sample. On the untreated PET surface, the 5-nm Ag films exhibited a grayish-blue color; in the areas irradiated at 308 nm with various numbers of pulses, the island films appeared uniformly blue. Irradiation at 248 nm resulted in more drastic ef-

fects; a black charred stripe was seen in the center of the irradiated area prior to any metal deposition. Upon evaporation of silver onto such a sample, a color variation was observed across the irradiated area. Proceeding from the circumference to the center, one passes through blue, white, and gray zones, to reach the black stripe in the center mentioned above.

SERS spectra have been recorded in all these zones, by focusing the laser onto different spots. Generally, a weaker surface enhancement, as well as the absence of any additional vibration bands, was observed. Differential changes in the relative SERS intensities of individual vibrations will be discussed below. Typical spectra recorded on irradiated surfaces are compared with the spectrum of an untreated film in Fig. 3. Irradiation with 100 pulses at 308 nm (100 mJ per pulse incident on an area of 2 cm^2 ; repetition rate 2 Hz; second trace from bottom) results in a modest decrease of band intensities and signal-to-noise ratio, as judged from the respective calibration bars. The effect of delivering 1000 pulses (308 nm) to the sample at a rate of 10 Hz is shown in the third trace of Fig. 3. Pulse repetition rates of ≥ 10 Hz are known to induce surface melting. In fact, the resulting spectrum is similar to the one of molten PET (top trace in Fig. 1); in particular, the strong fluorescence background is common to both spectra.

As the photon energy is increased by changing the wavelength to 248 nm (50 mJ per pulse, 1.0 cm^2 area), irradiation by 100 pulses gives rise to a much more severe deterioration of the spectrum, recorded in the white zone described above (top trace of Fig. 3). As the observed area is shifted, proceeding from the circumference to the center of the irradiated area, the signal-to-noise ratio of the PET-related bands in the spectra is observed to decrease, while a broad band at 1604 cm^{-1} , assigned to impurity species or decomposition products, increases in intensity.

UV-Visible Spectra of Ag Island Films on Laser-Treated PET. Upon 248-nm excimer laser irradiation, the initially clear PET foils became nontransparent and dark in color. In contrast, during 308-nm irradiation the samples turned slightly opaque only after 1000 pulses had been delivered to the sample at a 10-Hz rate. However, the absorption maximum of the silver island film deposited on top of the irradiated polymer surface experienced a pronounced red shift that increased with the number of pulses delivered to the surface, as shown in Fig. 4. The maximum, which is positioned at 552 nm on the untreated PET sample, shifts to 578, 590, and 643 nm on surfaces exposed to 10, 100, and 1000 excimer laser pulses, respectively.

Two factors can be identified that could give rise to such a shift, i.e., laser-induced changes in the polarity or in the morphology of the surface. To differentiate between these possibilities, we have performed contact angle measurements on the treated PET surfaces; the results are summarized in Fig. 5. The polar part of the surface energy decreases with the logarithm of the number of laser pulses at 308 nm. Simultaneously, the dispersive part exhibits an equal and opposite increase, so that the total surface energy remains approximately constant. (For the samples treated at 248 nm, analogous measurements were not possible, as the very rough sur-

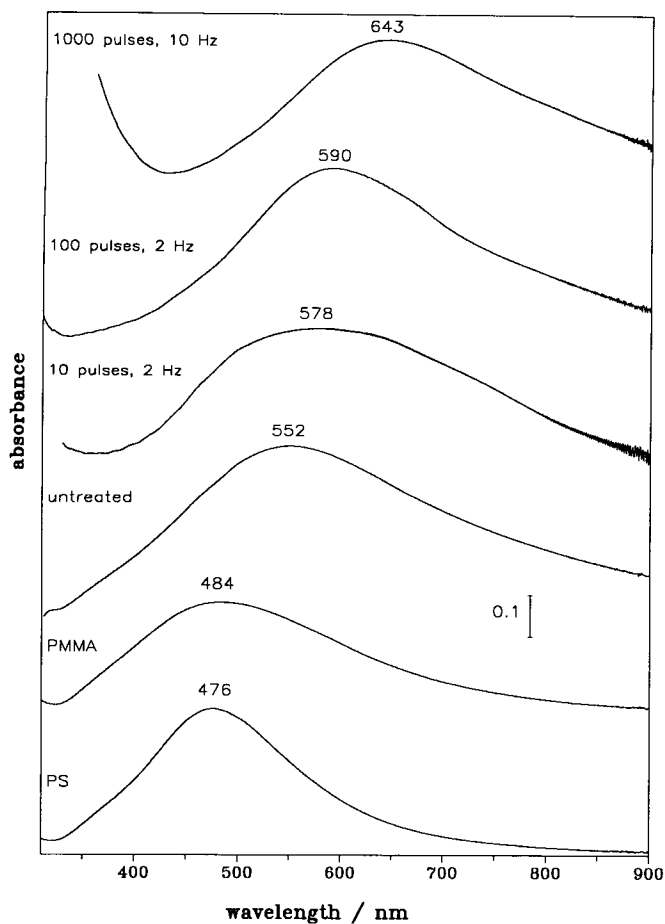


FIG. 4. Influence of excimer laser treatment on the visible absorption spectra of silver island films deposited on top of the irradiated PET samples. Irradiation conditions are the same as specified in Fig. 5. Absorption spectra deposited onto polystyrene and PMMA films are shown in the bottom two traces.

face impeded meaningful contact angle measurements.) In contrast, for 193-nm irradiation of PET, Lazare and Srinivasan²⁸ have reported that both the polar part and the total surface energy are decreasing.

Surface Structure of Laser-Treated PET Foils. Before discussing implications of the contact angle measurements on the interpretation of the observed red shift of the island film absorption, we must assess the *structural* changes induced by the excimer laser irradiation. Lazare *et al.*³⁵ have pointed out that these two factors may be closely related; i.e., surface roughening causes changes in the measured contact angles. The surface of PET, which originally exhibits glass-like smoothness, may be roughened in a controlled manner by 193-nm or 248-nm irradiation; the surface structures created have been related to the stretching direction and to the degree of crystallinity of the PET foils.

Results of irradiation of our samples at 308 nm are presented first. In a series of scanning electron micrographs recorded on 100- μ m-thick films exposed to 10, 100, and 1000 pulses, significant alterations of the surface morphology were observed only for the sample exposed to 1000 pulses at a repetition rate of 10 Hz (Fig. 6a). This extensive exposure gives rise to a change in visible color of the samples in the irradiated area, from colorless and

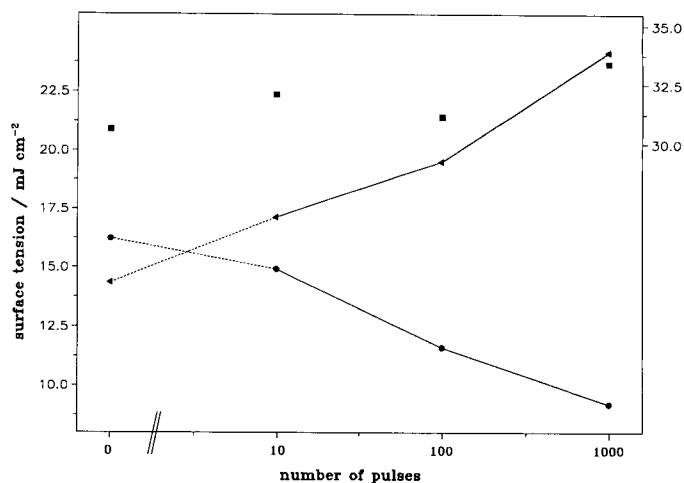


FIG. 5. Changes in the surface free energy of PET induced by laser irradiation. The polar (circles) and dispersive (triangles) components (both, left-hand scale), and the total surface energy (squares, right-hand scale) are displayed. The PET surfaces are characterized in the untreated state, and after exposure to 10, 100, and 1000 pulses of 100-mJ energy at 308 nm, incident onto an area of 2 cm².

transparent to opaque. The damaged surface layer of the polymer seen in Fig. 6a is indicative of thermal effects (i.e., surface melting), which are a consequence of the comparatively high repetition rate used.

Upon exposure to the 248-nm wavelength of the KrF* laser, periodic surface structures appeared, as documented in the micrographs of Fig. 6b and 6c. The excimer laser beam profile was not homogenized by spatial filtering, but the incident beam was unfocused onto the polymer samples; therefore, the intensity distribution is nonhomogeneous within the rectangular beam profile. The energy deposited within the irradiated area varied from low values at the edge to a maximum in the center. Near the circumference of the treated area, wavy structures were produced (Fig. 6b); towards the center conical structures are observed, with ejected material deposited on the tops of some of the cones (6c).

Several mechanisms for the formation of periodic surface structures in excimer laser irradiation experiments have been proposed in the literature. The presence of particulate impurities in the polymer films, as well as differences in the etch rates of crystalline and amorphous domains in stretched polymer samples, has been discussed.⁴⁶ Bahners and Schollmeyer⁴⁷ have attributed the appearance of surface ripples to a "synergetic effect" of Marangoni convection in the molten surface layer and of frozen-in stress fields which are released upon melting. However, pattern formation is also observed in non-melting polymers, such as polyimide.⁴⁸ To account for this observation, Tonyali *et al.*⁴⁹ state that release of the stress, which can be as high as 100 MPa, leads to the formation of microcracks, which become interconnected and thus give rise to a textured morphology. Dyer and Farley⁵⁰ have drawn attention to the importance of surface scattered waves. Niino and Yabe⁵¹ found indications that both the penetration depth of the laser into the polymer film and the thermal processes occurring on the surface during and after laser irradiation play a significant role in the formation of the microstructures. Recent

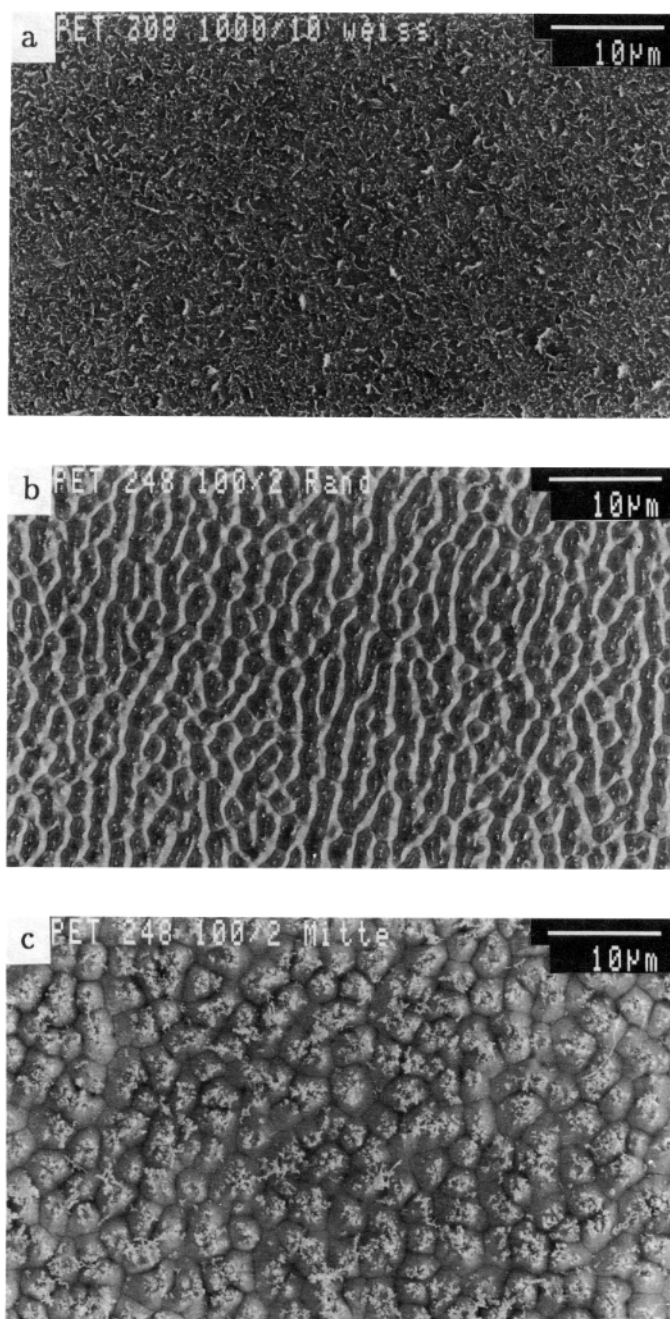


Fig. 6. Scanning electron micrographs of PET foil exposed to excimer laser irradiation at normal incidence: (a) 1000 pulses at 308 nm (100 mJ, 2 cm² area, rate 10 Hz); (b) 100 pulses at 248 nm (50 mJ, 1 cm² area, rate 2 Hz), edge of irradiated area; (c) 100 pulses at 248 nm (50 mJ, 1 cm² area, rate 2 Hz), center of irradiated area.

investigations⁴⁸ suggest that several of the mechanisms mentioned above may be acting simultaneously.

The scanning electron micrographs show not only the conical structures (also described as “naps”; see Fig. 6c) which are normally seen for biaxially stretched PET³⁵ but also wavy structures (6b) which are considered to represent the signature of monoaxially stretched PET. As a test for the origin of these structures, the angle of incidence of the laser beam was changed from normal to 45° and 60°, respectively; in addition, the sample was rotated by 90° around the surface normal.

The choice of a 60° incidence angle, at constant pulse energy, results in a reduction of laser fluence by a factor of 2. As a consequence, only scales or needle-type structures parallel to the surface are created, both at the edge (Fig. 7a) and at the center (7b) of the irradiated area. With 45° incidence, scaly structures with a larger distance between the walls ($\approx 3 \mu\text{m}$) are obtained near the edges of the irradiated area (Fig. 7c). In the center of the sample (7e), a scaly surface with ejected material is detected.

On the sample turned by 90° around the surface normal, the same types of morphological features are observed, with the direction of the waves and scales also rotated by 90° (Figs. 7d and 7f). In view of this result, the supplier was asked to provide details on the manufacturing of the biaxially oriented PET foils; it was confirmed that the two axes are not equivalent, but that the stress applied during production was higher in the transport direction of the foil. Thus it appears that the presence of anisotropic stress fields in the sample, and their release upon laser-induced melting and convection, would account for the three types of features observed on our PET samples (cones or naps on the one hand, and wavy structures resembling scales or needles on the other hand).

XPS Investigation of Laser-Irradiated and Silver-Decorated PET Surfaces. In the interpretation of the SERS spectra presented above, the formation of a bond between carbonyl groups of the polymer and the deposited silver has been considered. To obtain more information on the Ag/PET interface, we have recorded XPS spectra on as-received and laser-treated PET films, without and with deposited silver or gold island films. Results are shown in Fig. 8. Metal deposition results in an overall decrease in the intensity of the polymer spectral features, which demonstrates that the screening effect of the metal is large. However, substantial C 1s and O 1s signals are recorded also in the presence of a 5-nm silver island film, in spite of the fact that the escape depth of the corresponding photoelectrons does not exceed 5 nm. This is, of course, a consequence of the well-known grainy structure of the island films; in between the silver aggregates, of typical dimensions on the order of $\approx 20 \text{ nm}$, a large fraction of the surface is present with, at most, a low coverage of silver, i.e., below the resolution of the transmission electron microscope.⁵²

The XPS signal positions were calibrated with respect to the (hydrocarbon) C 1s signal at 284.7 eV. Composite peaks have been deconvoluted into the minimum number of Gaussian bands required for a satisfactory representation of the measured spectra. The results of the non-linear least-squares fits are included in Fig. 8; spectral parameters are compiled in Table II.

When comparing the spectrum of untreated PET (Fig. 8, top) with the spectrum of a sample irradiated at 308 nm, one notices only minor changes (cf. Table II). Changes induced by 248-nm irradiation are much more pronounced: The “hydrocarbon” signal at 284.7 eV (site 1 in Table II) and the peak at 289 eV (site 3) assigned to C=O^{53,54} appear significantly broadened, and the relative intensity of site 2 (binding energy 287 eV, corresponding to singly bound oxygen, C-O^{53,54}) is reduced.

Decoration of an untreated PET sample with a silver island film results in a loss of the C 1s shakeup satellite, a strong relative decrease of the signal due to carbonyl

TABLE II. XPS band positions and intensities.

Signal	PET untreated	PET untreated + 5 nm Ag	PET laser treated + 5 nm Ag	PET untreated + 5 nm Au	PET laser treated 308 nm	PET laser treated 248 nm	Ref. 53	Ref. 54
C 1s								
Site 1								
Position (eV)	284.7	284.7	284.7	284.7	284.7	284.7	284.7	284.6
FWHM (eV)	1.70	1.92	2.31	2.27	1.80	2.47	1.0	
Intensity (%)	73.8	73.5	76.2	73.8	63.6	76.5	59	
Site 2								
Position (eV)	286.4	287.5	287.3	286.9	286.6	287.0	286.2	286.1
FWHM (eV)	1.20	2.39	1.58	1.00	1.45	1.26	1.1	
Intensity (%)	12.1	16.6	11.3	6.7	18.5	6.1	22	
Site 3								
Position (eV)	288.6	289.2	288.9	288.8	288.8	289.0	288.7	288.6
FWHM (eV)	1.20	1.01	2.32	2.11	1.41	2.01	0.85	
Intensity (%)	14.1	1.3	12.5	19.5	17.9	17.4	19	
Site 4 (C-O-Ag)								
Position (eV)		282.5		
FWHM (eV)		2.16		
Intensity (%)		8.6		
Shake up								
Position (eV)	291.2	291.5	291.4		290.6
FWHM (eV)	2.0	2.30	2.35		
Intensity (%)	3.4	0.93	0.82	7	
O 1s								
Site 1								
Position (eV)	533.1	533.6	532.7	533.4	531.7	533.5	533.2	533.5
FWHM (eV)	1.75	2.33	3.29	1.73	1.77	2.04	1.31	
Intensity (%)	38.6	22.3	38.2	35.2	54.1	42.0	53	
Site 2								
Position (eV)	531.6	532.2	531.6	531.9	533.5	531.9	531.6	532.2
FWHM (eV)	1.84	1.37	3.60	1.91	1.91	2.20	1.19	
Intensity (%)	61.4	31.7	61.8	64.8	45.9	58.0	47	
Site 3 (O-Ag)								
Position (eV)	...	530.9	531.2
FWHM (eV)	...	2.33	
Intensity (%)	...	46.0	
I(O)/I(C)	1.072	0.403	0.503	0.493	0.846	0.646		

(C=O) centers, and a line broadening of all peaks. In addition, bands at new chemical shift positions are detected in both the O 1s and C 1s regions. The O 1s signal at 530.9 eV is attributed to oxygen bound to silver (O-Ag; cf. Ref. 40); similarly, the C 1s component at 282.5 eV may be attributed to a C \rightarrow O \cdots Ag center, by analogy with a similar chemical shift observed upon evaporation of aluminum onto PET.⁵⁵

The fifth trace in Fig. 8 shows the effect of silver deposition onto a 308-nm irradiated sample. We recall that for the laser-irradiated samples, much weaker SERS signals have been detected. It is therefore most remarkable that the O-Ag and C \rightarrow O \cdots Ag features are missing in the corresponding XPS spectra (Fig. 8e). A clear decrease of the oxygen functionalities of the polymer, as compared to the corresponding sample without silver, is seen by inspection of the intensity data in Table II.

The bottom set of spectra in Fig. 8 was recorded on a sample on which a gold island film had been deposited. No indications for the presence of an XPS band assignable to C \rightarrow O \cdots Au band are seen in the spectrum. This observation correlates with the fact that no SERS spectra

were observed with this sample either, and may be related to the instability of gold oxides, as mentioned above.

DISCUSSION

Possible origins for the astonishingly high surface enhancement observed with the PET foils are addressed first. We emphasize that the intensity of the SERS signals, as shown in Fig. 2, is usually observed only in surface-enhanced *resonance* Raman scattering (SERRS^{56,57}). One peculiarity of the samples used is the semicrystalline structure of the biaxially stretched PET foils. From polarized IR and density measurements on drawn PET samples, Orchard *et al.*⁴³ have concluded that the ethylene segments are present in the *trans* conformation in the crystalline domains. The axis connecting the two carbonyl substituents on the phenyl ring was found to be oriented approximately parallel to the surface, while the plane of the rings was tilted with respect to the plane of the surface. A reduction of this tilt angle was observed upon stretching or high-temperature annealing.⁴³ Upon both of these treatments, the degree of crystallinity is

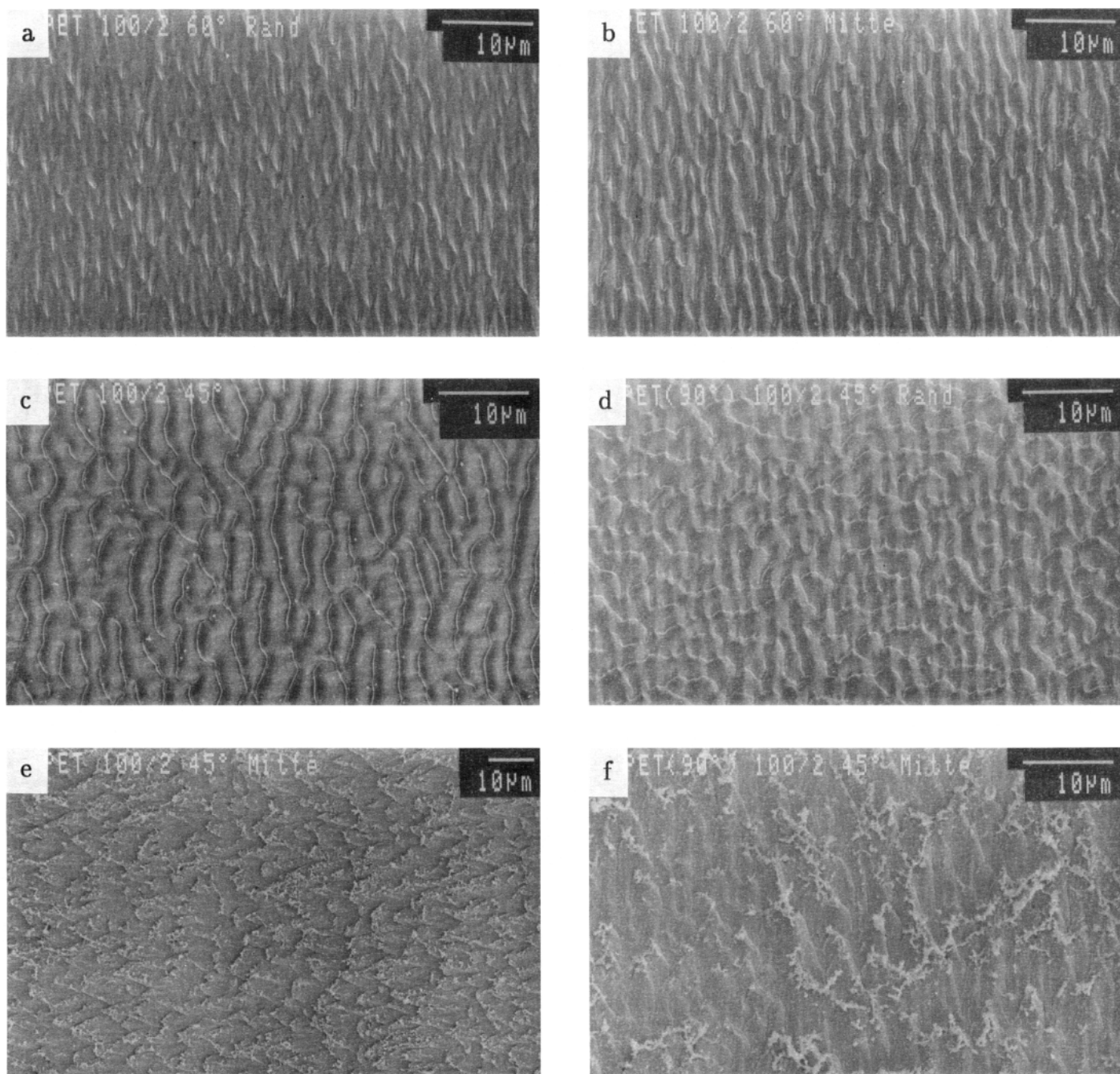


FIG. 7. Scanning electron micrographs of PET foil exposed to 248-nm excimer laser irradiation (100 pulses, 50 mJ, 1.0 cm² area, 2 Hz) at oblique incidence: (a) 60° angle of incidence, edge of irradiated area; (b) 60° angle of incidence, center of irradiated area; (c) 45° angle of incidence, edge of irradiated area; (d) same as c, but sample rotated by 90°; (e) 45° angle of incidence, center of irradiated area; (f) same as e, but sample rotated by 90°.

enhanced, and the phenyl rings reorient to approach an orientation parallel to the surface. A study of metal adhesion on PET is in agreement with these results; Silvain *et al.*⁵⁸ have given arguments that, in the semicrystalline material, the polymer main chains are oriented parallel to the surface. Carbonyl groups protruding out of the surface are providing preferred anchoring sites for impinging metal atoms.

Additional information on the orientation of the aromatic rings is obtained from relative band intensities in the SERS spectra. (We recall that electromagnetic surface selection rules^{59,60} should only be considered as qual-

itative guidelines for interpretation, due to the interfering effects of the chemical enhancement mechanism.²) The fact that several not-totally-symmetric in-plane stretching vibrations of the phenyl rings are strongly enhanced may be taken as an indication that the rings are not lying parallel to the surface in the virgin material. Rather, they are tilted out of the surface, with the CO-phenyl-CO-axis in the plane of the surface. Silvain *et al.*⁵⁸ have concluded that, upon melting, the rings tend to reorient into a position parallel to the surface. This interpretation is in agreement with our observation that SERS intensities decrease drastically upon melting.

Another reason for the exceptional role of PET might be the chemical contribution² to the SERS enhancement. The importance of a chemical bond is suggested by the absence of the C=O stretching frequency in the SERS spectra, and by the observation of an Ag-O band in XPS. For all samples where the latter band was not observed in XPS, the SERS spectra turned out to be weak. An additional chemical contribution might be provided by the formation of an Ag-phenyl complex, which would explain⁵⁴ the loss of the C 1s shape-up band for samples with deposited silver island films. (By comparison, with amorphous polystyrene only a small fraction of the phenyl rings is exposed on the surface⁶¹ and, therefore, in a position suitable for interaction with the deposited silver. This factor accounts for the weakness of the SERS signals observed for polystyrene.)

It has been pointed out⁶² that laser irradiation may induce melting of surface polymer layers, which may thereby become amorphous; this thermal effect is particularly pronounced with long-wavelength lasers. IR spectroscopic investigations of PET^{37,38} have shown the prevalence of all-*trans* chain conformations, which are characteristic for the crystalline state, on the untreated samples. Upon irradiation with a 248-nm KrF* laser, the conformation was observed to change into predominantly *gauche*, which is indicative of an amorphous state.³²

Furthermore, attention must be drawn to the silver deposition itself. The linewidth of the bands was observed to increase⁵⁴ upon silver deposition, due to thermal destruction of surface layers by the hot Ag atoms impinging on the surface.⁴⁰ In agreement with this argument, a significant line broadening is observed in our XPS spectra (fourth trace in Fig. 8; cf. Table II). Diffusion of the silver into subsurface regions is likely to be unimportant; for semicrystalline polymers, it has been shown⁶³ that diffusion processes are negligibly slow below the glass transition temperature.

In view of this evidence, it is important to discuss whether the changes observed on our samples as a consequence of laser irradiation are due to melting or to other nonthermal effects. Information from the SERS spectra is helpful in answering this question. The damage induced by silver deposition is not relevant to the SERS spectrum, as high-sensitivity spectra are recorded on silver-decorated virgin PET foils. On the other hand, transformation into the completely amorphous state has a drastic effect on the spectrum (Fig. 1, top). An intermediate case of partial amorphization (not shown) has been found with a resolidified bubble in a PET film; the appearance of a SERS spectrum recorded in this area lies in between those of virgin and of molten PET.

The SERS signals on silver-decorated, laser-irradiated samples are weaker by an overall factor of 1.5–2.3, as compared to the ones recorded on *virgin* PET foils. Thermal effects may be partly responsible for this decrease in intensity. However, the insensitivity of the SERS spectrum to the silver deposition process itself suggests that the changes in the SERS signals on irradiated surfaces are at least partly due to the laser-induced changes in surface structure and morphology. If, as a consequence of surface roughening, laser-induced crosslinking, or decreasing polarity of the surface, the adhesion of the islands is reduced, this result would also give rise to a

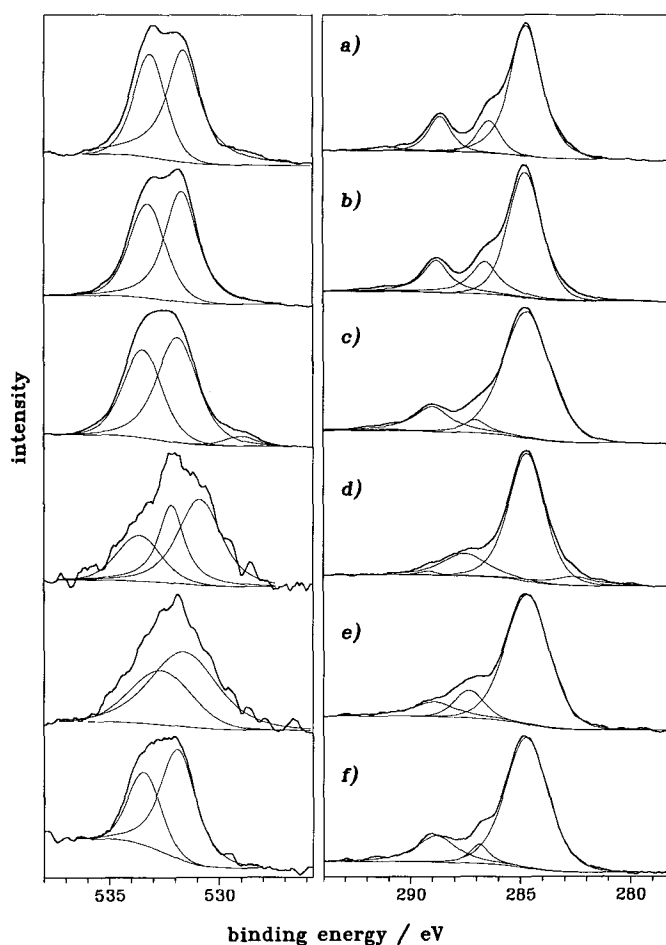


FIG. 8. XPS spectra of PET foils subject to various treatments. The O 1s (left) and C 1s (right) spectral regions are displayed for each sample. (a) Untreated PET; (b) PET exposed to 100 pulses at 308 nm; (c) PET exposed to 100 pulses at 248 nm; (d) untreated PET decorated with silver island film; (e) PET exposed to 100 excimer laser pulses at 308 nm, with subsequent deposition of silver island film; (f) untreated PET with gold island film.

decrease in the SERS signals of directly bound molecules. In addition, the observed changes in the island film absorption (Fig. 4) are expected to be paralleled by a change in the wavelength dependence of the SERS excitation profile. This effect has not yet been quantified due to problems with interfering fluorescence signals observed upon longer-wavelength (647 nm) excitation, and in view of difficulties associated with ageing of the island films.

For laser-treated PET, no *new* SERS bands that would be indicative of introduced functional groups have been detected. In an effort to assess any changes in relative band intensities, spectra have been normalized with respect to the intensity of the ring-breathing mode at 857 cm^{-1} , of symmetry A_g (Table I). When computing differences between the normalized spectra of irradiated and virgin PET foils, we find a decrease in the bands at 1235 and 1131 cm^{-1} involving C-O stretches, and an increase in the intensities of C-C-C and C-H out-of-plane deformational modes at 703 and 385 cm^{-1} , respectively. These changes suggest that, upon irradiation, the average tilt angle of the phenyl rings with respect to the surface is reduced, in agreement with the findings of Silvain *et*

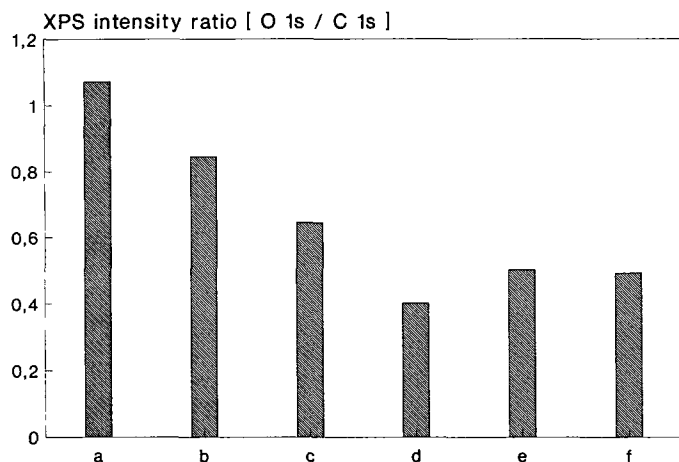


FIG. 9. Oxygen-to-carbon ratio derived from the corresponding peak areas of XPS core level signals. The labeling of the samples is the same as in Fig. 8, i.e., (a) untreated PET; (b) PET exposed to 100 pulses at 308 nm; (c) PET exposed to 100 pulses at 248 nm; (d) untreated PET decorated with silver island film; (e) PET exposed to 100 excimer laser pulses at 308 nm, with subsequent deposition of silver island film; (f) untreated PET with gold island film.

*al.*⁵⁸ One might also see indications of a loss of CO in the decreasing bands, although molecular decomposition is likely to give rise to more drastic modifications of the spectrum.

Changes in the absorption spectra of the deposited island films (Fig. 4) also exhibit the effects of both changes in surface polarity and surface roughness. In general, a decrease in surface polarity gives rise to a long wavelength shift of the absorption maximum. We recall that such a red shift indicates a higher eccentricity, i.e., a stronger deviation of the islands from spherical geometry.^{1,3,5} The islands, which are commonly modeled as oblate spheroids, will tend to spread out on the surface and hence become flatter if the interfacial energy between silver and the surface is low, or else if a preformed morphology on the surface favors the formation of eccentric particles. As discussed above, PET provides favorable Ag-O anchoring sites; a low PET/silver interfacial energy appears to be the reason for the red shift of the absorption maximum on PET, by ≈ 70 nm, as compared to the highly polar PMMA surface (Fig. 4).

As the PET foils are irradiated, the polar part of the surface energy further decreases; in addition, a structuring of the surface has been shown to occur for exposure to 1000 pulses at 308 nm. The influence of the polarity appears to be most important, as the absorption maximum is observed to shift further towards the red upon irradiation (upper traces in Fig. 4).

The absorption spectrum of the silver islands deposited onto polystyrene (Fig. 4, bottom) is characterized by a short-wavelength absorption maximum at 476 nm. This observation is attributed to the extreme roughness and irregularity of the extrusion molded technical plaques, and to the possible influence of surface-segregated additives.

From the contact angle measurements, a decrease in the polar part of the surface energy was derived. The decrease in the oxygen-to-carbon ratio observed by XPS (Table II) is consistent with a loss of CO and CO₂, in

agreement with the results of other authors.^{28,64} Loss of the carbonyl anchoring sites might also be a reason for the decreasing SERS intensities.

A survey of the observed changes in the O/C ratio is given in Fig. 9. From the result that this ratio decreases with 308-nm treatment for pulse fluences of 50 mJ cm⁻², i.e., well below the threshold for ablation (170 mJ cm⁻²), Dyer *et al.*³³ have inferred a preferential loss of C=O. The stronger additional decrease of the O/C ratio after excimer laser treatment at 248 nm above the ablation threshold is attributed to losses of both C=O and CO₂. In this respect, the present results are in agreement with those of Kokai *et al.*³¹ and with a series of investigations at the excimer wavelengths of 193, 248, and 308 nm.^{28,30,31,33,64} A contradictory result has been reported by Schollmeyer and co-workers.³²

After metal deposition the O/C ratio is observed to decrease drastically (cf. Fig. 9a and d). Chtaib *et al.*²⁷ have attributed this observation to the island-like growth of the metal. A possible additional reason for the decreasing O/C ratio is the deposition of carbonaceous species from the atmosphere onto freshly evaporated silver island films.^{65,66}

Interestingly, metal deposition on a laser-irradiated PET sample has a less pronounced effect (Fig. 9b and 9e). The O/C ratio after silver deposition on the irradiated sample (9e) is even somewhat higher than on the virgin Ag-decorated PET (9d). We have argued above that laser treatment at 308 nm induces a loss of surface C=O groups, and reduces the orientation of the C=O groups relative to the surface, as a consequence of thermally induced amorphization. As the oxygen functional groups are no longer preferentially orientated perpendicular to the surface, where they would be covered by growing Ag clusters, the O/C ratio is reduced to a lesser extent by metal deposition.

The XPS results obtained with Au deposition demonstrate that no Au-O bonds are formed, from the absence of a corresponding chemical shift in either carbon or oxygen signals. Yet, the Au clusters appear to preferentially screen the oxygen, as the O/C ratio is reduced for this sample as well. We note that, in spite of a higher Au thickness, the decrease in O/C is not as high as that observed with Ag, where a definite Ag-O bond has been shown to be formed. Taken together, these observations also suggest that the Au island films start to grow in the vicinity of C=O anchoring sites, even though the precise type of interaction has not yet been established.

CONCLUSIONS

The unusually strong SERS intensities observed on silver-decorated PET foils have been attributed to a specific orientation of the polymer chains at the surface of the stretched, semicrystalline material. Excimer laser irradiation at fluences well below the ablation threshold results in a loss of surface carbonyl groups. This process has been established from XPS spectra, contact angle measurements, shifts in the absorption spectra of deposited silver island films, and changes in the SERS spectra. Surface melting has been identified as a second cause for the decrease in SERS intensities on irradiated samples; the surface structuring, as visualized by electron

microscopy, reveals the influence of strain fields generated during stretching of the polymer foils, which are partly released upon laser-induced melting.

With regard to the SERS spectra, all available evidence indicates that the principal effect of laser irradiation of the PET foils is a reduction in the silver/polymer bonding. This interpretation is in agreement with the results on gold-decorated PET films, where no Au-O or Au-O-C bands were detected in the XPS spectra, and concurrently no SERS spectra could be detected. In future work, the study will be complemented by decoration with Cu island films; bonding of this metal to polymer surfaces has been established in the literature.²⁷

ACKNOWLEDGMENTS

The authors are indebted to D. Hubbert, who performed several experiments on the silver decoration of polystyrene samples. Financial support by the Deutsche Forschungsgemeinschaft (SFB 213) is gratefully acknowledged.

1. R. K. Chang and T. E. Furtak, *Surface Enhanced Raman Scattering* (Plenum, New York, 1984).
2. A. Otto, in *Light Scattering in Solids*, M. Cardona and G. Güntherodt, Eds. (Springer, Berlin, 1984), Vol. 4, Chap. 6; A. Otto, I. Mrozek, H. Grabhorn, and W. Akemann, *J. Phys.: Condens. Matter* **4**, 1143 (1992).
3. M. Moskovits, *Rev. Mod. Phys.* **57**, 783 (1985).
4. K. Arya and R. Zeyher, in *Light Scattering in Solids*, M. Cardona and G. Güntherodt, Eds. (Springer, Berlin, 1984), Vol. 4, Chap. 6.
5. A. Wokaun, *Solid State Phys.* **38**, 223 (1984); A. Wokaun, *Mol. Phys.* **56**, 1 (1985).
6. R. Aroca and G. J. Kovacs, in *Vibrational Spectra and Structure*, J. R. Durig, Ed. (Elsevier, Amsterdam, 1991), Vol. 19, p. 55.
7. D. J. Jeanmaire and R. P. Van Duyne, *J. Electroanal. Chem.* **84**, 1 (1977).
8. H. R. Virdee and R. E. Hester, *Croat. Chem. Acta* **61**, 357 (1988); H. R. Virdee and R. E. Hester, *Laser Chem.* **9**, 401 (1988).
9. R. Holze, *Electrochim. Acta* **35**, 1037 (1990); *ibid.* **36**, 1523 (1991); R. Holze, *Z. Phys. Chem.* **160**, 45 (1988).
10. P. C. Lee and D. Meisel, *Chem. Phys. Lett.* **99**, 262 (1983).
11. J. S. Suh and K. H. Michaelian, *J. Raman Spectrosc.* **18**, 409 (1987).
12. D. L. Allara, C. A. Murray, and S. Bodoff, in *Physicochemical Aspects of Polymer Surfaces*, K. L. Mittal, Ed. (Plenum, New York, 1983), Vol. 1, p. 33.
13. P. G. Roth and F. J. Boerio, *J. Polym. Sci.: Polym. Phys. Ed.* **25**, 1923 (1987).
14. D. B. Parry and A. L. Dendramis, *Appl. Spectrosc.* **40**, 656 (1986).
15. R. S. Venkatachalam, F. J. Boerio, M. R. Carnevale, and P. G. Roth, *Appl. Spectrosc.* **42**, 1207 (1988).
16. H. Ishida, H. Fukuda, G. Katagiri, and A. Ishitani, *Appl. Spectrosc.* **40**, 322 (1986).
17. Y. Nishikawa, Y. Ito, K. Fujiwara, and T. Shima, *Appl. Spectrosc.* **45**, 752 (1991).
18. Y. Mo, H. von Känel, and P. Wachter, *Solid State Commun.* **52**, 213 (1984).
19. R. P. Van Duyne, J. P. Haushalter, M. Janik-Czachor, and N. Levinger, *J. Phys. Chem.* **89**, 4055 (1985).
20. B. B. Kaul, R. E. Holt, V. L. Schlegel, and T. M. Cotton, *Anal. Chem.* **60**, 1580 (1988).
21. R. W. Chantrell and K. O'Grady, *J. Phys.* **D25**, 1 (1992).
22. J. Heitz, E. Arenholz, T. Kefer, D. Bäurele, H. Hibst, and A. Hagemeyer, *Appl. Phys.* **A55**, 391 (1992).
23. J. E. Andrew, P. E. Dyer, R. D. Greenough, and P. H. Key, *Appl. Phys. Lett.* **43**, 1076 (1983).
24. S. Lazare, V. Granier, P. Lutgen, and Y. Novis, *Chemtronics* **4**, 157 (1989).
25. J. F. Sylvain, A. Veyrat, and J. J. Ehrhardt, in *Polymer-Solid Interfaces*, J. J. Pireaux, P. Bertrand, and J. L. Bredas, Eds. (IOP Publ., Bristol, 1992), p. 281.
26. J. F. Sylvain, A. Arzur, M. Alnot, J. J. Ehrhardt, and P. Lutgen, *Surf. Sci.* **251**, 787 (1991).
27. M. Chtaib, J. Ghijsen, J. J. Pireaux, and R. Caudano, *Phys. Rev. B* **44**, 10815 (1991).
28. S. Lazare and R. Srinivasan, *J. Phys. Chem.* **90**, 2124 (1986).
29. R. Srinivasan and S. Lazare, *Polymer* **26**, 1297 (1985).
30. M. Chtaib, E. M. Roberfroid, Y. Novis, J. J. Pireaux, R. Caudano, P. Lutgen, and G. Feyder, *J. Vac. Sci. Technol.* **A7**, 3233 (1989).
31. F. Kokai, H. Saito, and T. Fujioka, *Macromolecules* **23**, 674 (1990).
32. T. Bahners, D. Knittel, F. Hillenkamp, U. Bahr, C. Benndorf, and E. Schollmeyer, *J. Appl. Phys.* **68**, 1854 (1990).
33. P. E. Dyer, G. A. Oldershaw, and J. Sidhu, *J. Phys. Chem.* **95**, 10004 (1991).
34. G. A. Oldershaw, *Chem. Phys. Lett.* **186**, 23 (1991).
35. S. Lazare, V. Granier, P. Lutgen, and G. Feyder, *Rev. Phys. Appl.* **23**, 1065 (1988).
36. Y. Novis, R. DeMeulemeester, M. Chtaib, J. J. Pireaux, and R. Caudano, *Brit. Polym. J.* **21**, 147 (1989).
37. I. M. Ward and M. A. Wilding, *Polymer* **18**, 327 (1977).
38. T. R. Manley and D. A. Williams, *Polymer* **10**, 339 (1969).
39. J. Purvis and D. J. Bower, *J. Polym. Sci.: Polym. Phys. Ed.* **14**, 1461 (1976).
40. M. C. Tobin, *J. Phys. Chem.* **61**, 1392 (1957).
41. D. A. Weitz, S. Garoff, J. Gersten, and A. Nitzan, *J. Chem. Phys.* **78**, 5324 (1983).
42. J. A. Creighton, in *Spectroscopy of Surfaces*, R. J. H. Clark and R. E. Hester, Eds. (Wiley, Chichester, 1988), Vol. 16, p. 37.
43. G. A. J. Orchard, P. Spiby, and I. M. Ward, *J. Polym. Sci. Polym. Phys. Ed.* **28**, 603 (1990).
44. R. Srinivasan and B. Braren, *Chem. Rev.* **89**, 1303 (1989).
45. S. Lazare and V. Granier, *Laser Chem.* **10**, 25 (1989).
46. Y. Novis, J. J. Pireaux, A. Brezini, E. Petit, R. Caudano, P. Lutgen, G. Feyder, and S. Lazare, *J. Appl. Phys.* **64**, 365 (1988).
47. T. Bahners and E. Schollmeyer, *J. Appl. Phys.* **66**, 1884 (1989).
48. E. Arenholz, M. Wagner, J. Hertz, and D. Bäuerle, *Appl. Phys.* **A55**, 119 (1992).
49. K. Tonyali, L. C. Jensen, and J. T. Dickinson, *J. Vac. Sci. Technol.* **A6**, 941 (1988).
50. P. E. Dyer and R. J. Farley, *Appl. Phys. Lett.* **57**, 765 (1990).
51. H. Niino and A. Yabe, *J. Photochem. Photobiol. A: Chem.* **65**, 303 (1992).
52. R. Möller, C. Baur, U. Graf, P. Kürz, A. Leitner, J. D. Pedarnig, and F. R. Aussenegg, *J. Phys. D: Appl. Phys.* **23**, 1267 (1990).
53. G. Beamson and D. Briggs, in *High Resolution XPS of Organic Polymers* (Wiley, Chichester, 1992), p. 174.
54. L. J. Gerenser, *J. Vac. Sci. Technol.* **A8**, 3682 (1990).
55. Q. T. Le, M. Chtaib, J. J. Pireaux, and R. Caudano, in *Polymer-Solid Interfaces*, J. J. Pireaux, P. Bertrand, and J. L. Bredas, Eds. (IOP Publ., Bristol, 1992), p. 245.
56. D. L. Jeanmaire and R. P. Van Duyne, *J. Electroanal. Chem.* **84**, 1 (1977); T. M. Cotton, S. G. Schultz, and R. P. Van Duyne, *J. Am. Chem. Soc.* **104**, 6528 (1982).
57. P. Hildebrandt and M. Stockburger, *J. Phys. Chem.* **88**, 5935 (1984).
58. J. F. Sylvain, A. Veyrat, and J. J. Ehrlich, *Thin Solid Films* **221**, 114 (1992).
59. M. Moskovits, *J. Chem. Phys.* **77**, 4408 (1982).
60. J. A. Creighton, in *Spectroscopy of Surfaces*, J. H. Clark and R. E. Hester, Eds. (Wiley, Chichester, 1988), p. x-x.
61. R. Rei Vilar, M. Schott, J. J. Pireaux, C. Gregoire, P. A. Thiry, R. Caudano, A. Lapp, A. M. Bothelo do Rego, and J. Lopes da Silva, *Surface Sci.* **189**, 927 (1987).
62. G. Koren and J. T. C. Yeh, *J. Appl. Phys.* **56**, 2120 (1984).
63. F. Faupel, in *Polymer-Solid Interfaces*, J. J. Pireaux, P. Bertrand, and J. L. Bredas, Eds. (IOP Publ., Bristol, 1992), p. 171.
64. S. Lazare, P. D. Hoh, J. M. Baker, and R. Srinivasan, *J. Am. Chem. Soc.* **106**, 4283 (1984).
65. J. C. Tsang, J. C. Demuth, P. N. Sanda, and J. R. Kirtley, *Chem. Phys. Lett.* **76**, 54 (1980).
66. M. R. Mahoney, M. W. Howard, and R. P. Cooney, *Chem. Phys. Lett.* **71**, 59 (1980); R. P. Cooney, M. R. Mahoney, and M. W. Howard, *Chem. Phys. Lett.* **78**, 404 (1981).